ORIGINAL ARTICLE

Microfibrillar-associated protein 4 modulates airway smooth muscle cell phenotype in experimental asthma

Bartosz Pilecki,[1] Anders Schlosser,[1] Helle Wulf-Johansson,[1] Thomas Trian,[2] Jesper B Moeller,[1] Niels Marcussen,[3] Juan A Aguilar-Pimentel,[4,5] Martin Hrabe de Angelis,[4,6] Jorgen Vestbo,[7,8] Patrick Berger,[2,9] Uffe Holmskov,[1] Grith L Sorensen[1]

▶ Additional material is published online only. To view please visit the journal online (http://dx.doi.org/10.1136/thoraxjnl-2014-206609).

For numbered affiliations see end of article.

Correspondence to
Dr Grith L Sorensen, Institute of Molecular Medicine, J.B. Winslows Vej 25.3, Odense C 5000, Denmark; glsorensen@health.sdu.dk

Received 21 November 2014
Revised 19 May 2015
Accepted 20 May 2015
Published Online First 2 June 2015

ABSTRACT

Background Recently, several proteins of the extracellular matrix have been characterised as active contributors to allergic airway disease. Microfibrillar-associated protein 4 (MFAP4) is an extracellular matrix protein abundant in the lung, whose biological functions remain poorly understood. In the current study we investigated the role of MFAP4 in experimental allergic asthma.

Methods MFAP4-deficient mice were subjected to alum/ovalbumin and house dust mite induced models of allergic airway disease. In addition, human healthy and asthmatic primary bronchial smooth muscle cell cultures were used to evaluate MFAP4-dependent airway smooth muscle responses.

Results MFAP4 deficiency attenuated classical hallmarks of asthma, such as eosinophilic inflammation, eotaxin production, airway remodelling and hyperresponsiveness. In wild-type mice, serum MFAP4 was increased after disease development and correlated with local eotaxin levels. MFAP4 was expressed in human bronchial smooth muscle cells and its expression was upregulated in asthmatic cells. Regarding the underlying mechanism, we showed that MFAP4 interacted with integrin αvβ5 and promoted asthmatic bronchial smooth muscle cell proliferation and CCL11 release dependent on phosphatidyloinositol-3-kinase but not extracellular signal-regulated kinase pathway.

Conclusions MFAP4 promoted the development of asthmatic airway disease in vivo and pro-asthmatic functions of bronchial smooth muscle cells in vitro. Collectively, our results identify MFAP4 as a novel contributor to experimental asthma, acting through modulation of airway smooth muscle cells.

Key messages

What is the key question?
- Here we investigated the role of MFAP4 in experimental asthma.

What is the bottom line?
- This study shows for the first time that MFAP4 is involved in the pathophysiology of asthmatic airway disease as a modulator of airway smooth muscle biology.

Why read on?
- The study identifies a novel pathway involved in bronchial smooth muscle cell modulation in asthma pathogenesis.

INTRODUCTION

Asthma is a chronic airway disease characterised by eosinophilic inflammation, airway hyperresponsiveness (AHR) and airway remodelling, and the interplay between these three components is still incompletely understood. Common features of asthmatic remodelling include changes in the composition of the extracellular matrix (ECM) as well as airway smooth muscle (ASM) hyperplasia and hypertrophy.[1] ASM interactions with the surrounding ECM have been demonstrated to be involved in ASM thickening. ECM components, and matrix derived from subjects with asthma, have been shown to increase healthy ASM proliferation.[2 3] Thus, changes in ECM composition and quantity may influence the function of neighbouring ASM cells.

The ASM–ECM interaction is mediated mainly through specific integrin receptors. Function-blocking studies have shown that β1 and αvβ3 integrins are responsible for fibronectin-mediated ASM proliferation and IL-1β-dependent cytokine production.[2 4] Moreover, an RGD-containing blocking peptide has been shown to attenuate ASM remodelling in a guinea pig asthma model, underlining the importance of integrin signalling in asthma in vivo.[5] The integrin-ligand interaction activates focal adhesion kinase (FAK) and further signal transduction, such as phosphatidyloinositol-3-kinase (PI3K) and extracellular signal-regulated kinase (ERK) pathways.[6]

Microfibrillar-associated protein 4 (MFAP4) is an ECM protein of the fibrinogen-related protein superfamily highly expressed in elastin-rich tissues, such as heart and lung.[7] Due to elastin-binding properties, MFAP4 was suggested to contribute to elastogenesis and maintenance of the proper structure of elastic fibres.[8 9] Importantly, MFAP4 contains an RGD sequence, suggesting that it can signal through integrin receptors, and we have shown that

To cite: Pilecki B, Schlosser A, Wulf-Johansson H, *et al*. *Thorax* 2015;**70**:862–872.

MFAP4 promotes vascular smooth muscle cell (SMC) proliferation and migration through integrins αvβ3 and αvβ5in vitro and in vivo (manuscript under revision). MFAP4 has also been suggested as a potential biomarker and, together with another ECM protein fibulin-5, as a contributor to abnormal tissue repair in COPD.[10 11] Furthermore, we have recently shown that MFAP4-deficient mice exhibit mild age-dependent emphysema-like airspace enlargement.[12]

In the present study, we investigated the potential role of MFAP4 in the development of allergic asthma using two distinct murine models. Furthermore, we examined if effects of MFAP4 could be explained by ASM phenotypic modulation using in vitro culture of human bronchial SMCs (BSMCs).

METHODS

Additional details on the methods are provided in the online supplementary material.

Mice

Female 8–12-week-old *Mfap4*$^{-/-}$(knockout, KO) mice, generated previously (manuscript under revision), and littermate *Mfap4*$^{+/+}$ (wild-type, WT) mice, were bred into the BALB/c background for more than 10 generations. The animals had access to pelleted chow and water ad libitum. The Danish National Animal Ethics Committee approved all animal experiments (permit 2012-15-2934-00354).

Allergic asthma models

Mice were sensitised intraperitoneally with 200 µg ovalbumin (OVA; grade VI) and 2 mg alum in 200 µL phosphate-buffered saline (PBS) on days 0 and 7. On days 14–16, mice were challenged intranasally with 20 µg OVA in 50 µL PBS under light isoflurane anaesthesia. Alum-sensitised, PBS-challenged mice were used as controls.

Alternatively, mice were challenged intranasally with 25 µg house dust mite extract total protein (HDM, endotoxin content 51.5 EU/mg protein) 5 days/week for 7 weeks as described previously.[13] PBS-treated mice were used as controls.

Twenty-four hours after the last exposure mice were anaesthetised and subjected to AHR measurements. Briefly, mice were tracheostomised and connected to the ventilator (Flexivent, SCIREQ) and lung function parameters were measured in the steady state and after exposure to nebulised methacholine (MCh). Immediately afterwards mice were sacrificed and blood, bronchoalveolar lavage (BAL) fluid and lungs were collected. Serum IgE levels were determined by ELISA. Cytokine levels were quantified in BAL and lung homogenates. Hydroxyproline content was measured in lung homogenates.

Lung histology

Formalin-fixed, paraffin-embedded lung tissues were cut in 4 -µm-thick slides and stained with H&E, periodic acid-Schiff (PAS), Picrosirius Red (PSR), or immunostained against α-smooth muscle actin (α-SMA) or MFAP4. The degree of inflammation, mucus production, fibrosis and ASM deposition was quantified by morphometric analysis.

Human subjects

Seven patients with severe persistent asthma and eight subjects without asthma were prospectively recruited from the CHU Bordeaux Teaching Hospital, Bordeaux, France, according to the Global Initiative for Asthma criteria.[14] All subjects gave their written informed consent to participate in the study, after the nature of the procedure had been fully explained. The study followed recommendations outlined in the Helsinki declaration and received approval from the local ethics committee. Bronchial specimens from all subjects were obtained by either fiberoptic bronchoscopy or lobectomy, as previously described.[15]

Cell culture

Primary human BSMCs derived from healthy or asthmatic donors (Lonza) were cultured in Dulbecco's Modified Eagle's Medium (DMEM) supplemented with 10% fetal bovine serum (FBS), 50 U/mL penicillin, 50 µg/mL streptomycin and 2 mM L-glutamine. Cells between passages 5 and 10 were used in all experiments.

BSMCs were further isolated from bronchial specimens as described previously.[15] Patient characteristics are presented in online supplementary table S1. Cells were cultured in DMEM supplemented with 10% FBS, 100 U/mL penicillin, 100 mg/mL streptomycin, 0.25 mg/mL amphotericin B, 2 mM L-glutamine, 1 mM sodium pyruvate and 1% non-essential amino acid mixture. Confluent cells were collected after 6–8 weeks. Cell purity and phenotype were validated by α-SMA and calponin positivity. Cells between passages 2 and 5 were used.

Real-time PCR

Relative expression of target genes was measured using Taqman Gene Expression Assays.

Detection of soluble MFAP4

MFAP4 levels in animal samples and BSMC lysates (prepared in PBS) were measured by AlphaLISA as described previously[7] and shown as U/mL. 1 U/mL corresponds to 38 ng/mL in human serum.

Adhesion assays

Cell adhesion to ECM coating with or without pretreatment with either RGD and DGR-containing peptides or anti-integrin antibodies was measured using Vybrant Cell Adhesion Assay Kit.

Proliferation assay

Serum-starved BSMCs were seeded in serum-free DMEM on ECM-coated plates and incubated for 48 h. Cell proliferation was assessed using bromodeoxyuridine (BrdU) incorporation assay.

In some experiments, cells were seeded in serum-free DMEM for 4 h to allow attachment. Subsequently, anti-integrin antibodies or inhibitors of PI3K and mitogen-activated protein kinase (MEK) (LY294002 and PD98059, respectively) were added for the rest of the incubation period. Isotype control antibody and DMSO were used as controls for anti-integrin antibodies and inhibitors, respectively.

Western blotting

Serum-starved cells were incubated for various time points in serum-free DMEM and lysed in RIPA buffer with protease and phosphatase inhibitors. Equal amounts of total protein samples were separated by SDS-PAGE and blotted with antibodies against GAPDH, integrin αv, integrin β5, pFAK (T397) or FAK.

Statistics

Statistical analysis was performed in Prism 5 software (GraphPad, La Jolla, California, USA). Data are presented as means+SEM unless stated otherwise. Normality of the data was checked using D'Agostino-Pearson test. Parametric results were analysed using Student's t test or either one-way or two-way analysis of variance (ANOVA) followed by Bonferroni's multiple

comparisons test. Non-parametric results were analysed using Mann–Whitney test. Correlations were analysed using Pearson's test. A value of $p<0.05$ was considered significant.

RESULTS

Circulating MFAP4 levels are increased in allergic asthma

In this study we used two models of experimental asthma: an OVA-induced sensitisation and challenge model and a model of prolonged exposure to a clinically relevant allergen, HDM. Histological analysis revealed MFAP4 localisation within the basement membrane, in close proximity to airway epithelial cells and SMCs (figure 1A). MFAP4 mRNA expression did not change after OVA or HDM treatment (figure 1B). However, upon challenge the concentration of soluble MFAP4 was significantly increased in serum of WT mice (figure 1C). Moreover, we found that MFAP4 levels were raised in BAL of HDM-treated WT mice (figure 1D), with a corresponding decrease of MFAP4 content in lung homogenate (figure 1E).

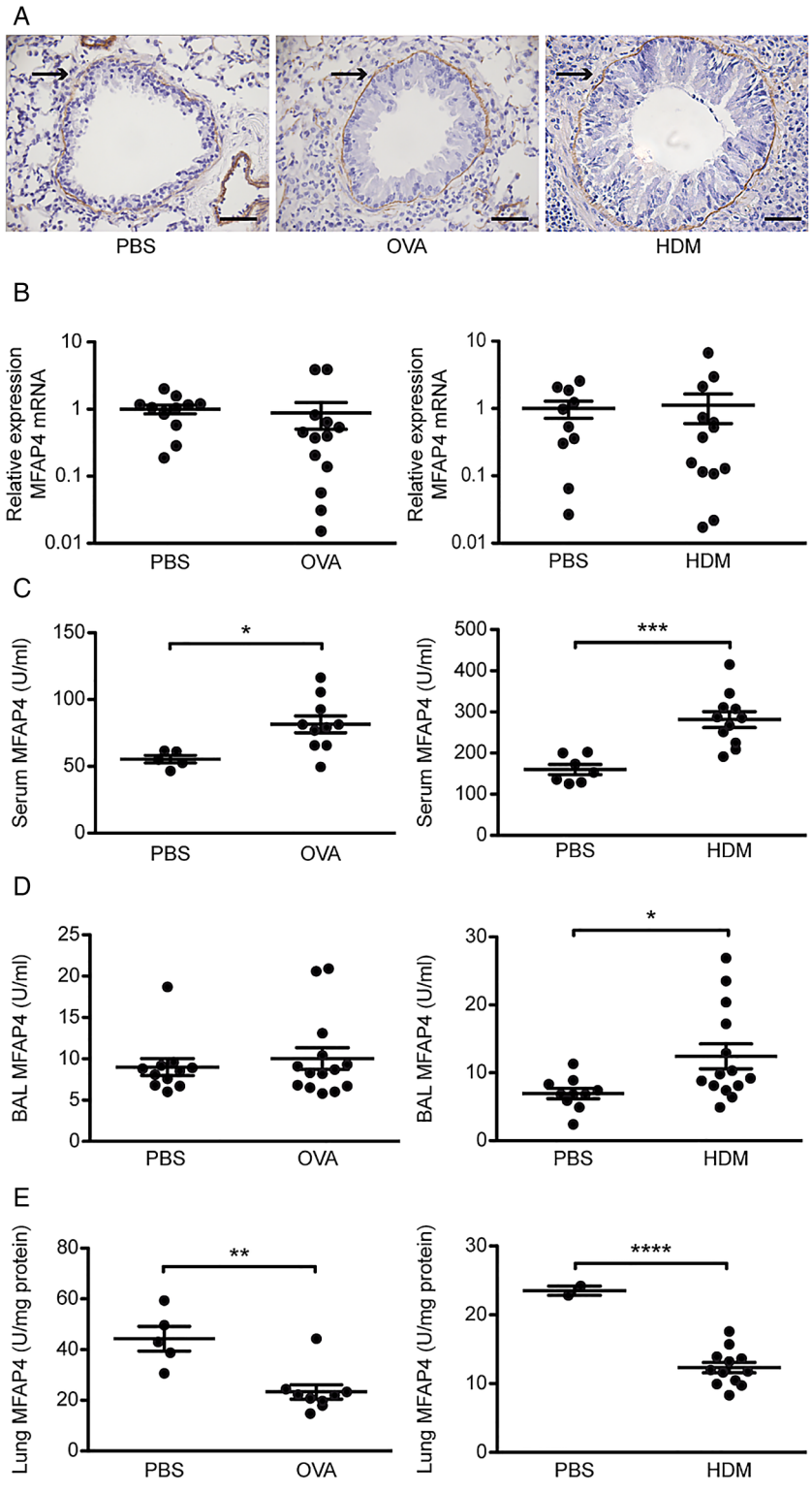

Figure 1 Microfibrillar-associated protein 4 (MFAP4) is increased in bronchoalveolar lavage (BAL) and serum of allergic mice. (A) Pulmonary localisation of MFAP4 in ovalbumin (OVA) and house dust mite (HDM) treated mice. MFAP4 staining is shown with arrows. (B) MFAP4 mRNA expression level in the lung after OVA and HDM exposure. (C and D) MFAP4 levels are changed in asthma. MFAP4 concentrations were measured after OVA and HDM exposure in (C) serum, (D) BAL and (E) lung homogenate. Scale bar, 50 μm. n=2–14. *p<0.05, **p<0.01, ***p<0.001, ****p<0.0001, calculated by Student's t test or Mann–Whitney test. PBS, phosphate-buffered saline.

MFAP4 deficiency attenuates allergy-induced airway eosinophilia and production of eotaxins

In both OVA and HDM models, MFAP4 KO mice showed decreased total cell and eosinophil numbers in BAL compared with WT littermates (figure 2A). The same pattern was observed in the lung parenchyma of OVA-treated mice, where WT animals exhibited more severe inflammation than their MFAP4-deficient counterparts (figure 2B, C). A trend towards reduced inflammation in the parenchyma was also observed in HDM-challenged MFAP4 KO mice (figure 2C). Moreover, we found a significant positive correlation between BAL eosinophil number and MFAP4 serum concentration in WT mice (figure 2D, E).

We then analysed the levels of CCL11 (eotaxin-1) and CCL24 (eotaxin-2), the chemokines essential for eosinophil recruitment. We found that OVA-treated MFAP4 KO mice had reduced amounts of CCL11 and CCL24 in BAL as well as in lung homogenates (figure 3A, B). Furthermore, the levels of lung CCL11 and CCL24 correlated with serum MFAP4 concentrations (figure 3C, D).

MFAP4 influences IL-13 production

Th2 cytokine production was analysed in BAL and lung homogenates of OVA-treated mice. The levels of IL-4 and IL-5 did not differ between challenged WT and KO animals (see online supplementary figure S1A, B). However, we observed reduced production of IL-13 in BAL and lung homogenates of MFAP4-deficient mice (see online supplementary figure S1C). Serum OVA-specific IgE levels remained unchanged between treated groups (see online supplementary figure S2). Thus, in the used models MFAP4 did not appear to play an essential role in regulating Th2 responses but promoted IL-13 production.

Lack of MFAP4 attenuates goblet cell metaplasia

To determine whether mucus production was affected by MFAP4, lung sections were stained with PAS to evaluate the number of mucus-producing goblet cells (figure 4A). MFAP4 deficiency in OVA-treated mice resulted in a significant decrease in goblet cell number (figure 4B). We confirmed our observations in the chronic HDM model, where MFAP4 deficiency also

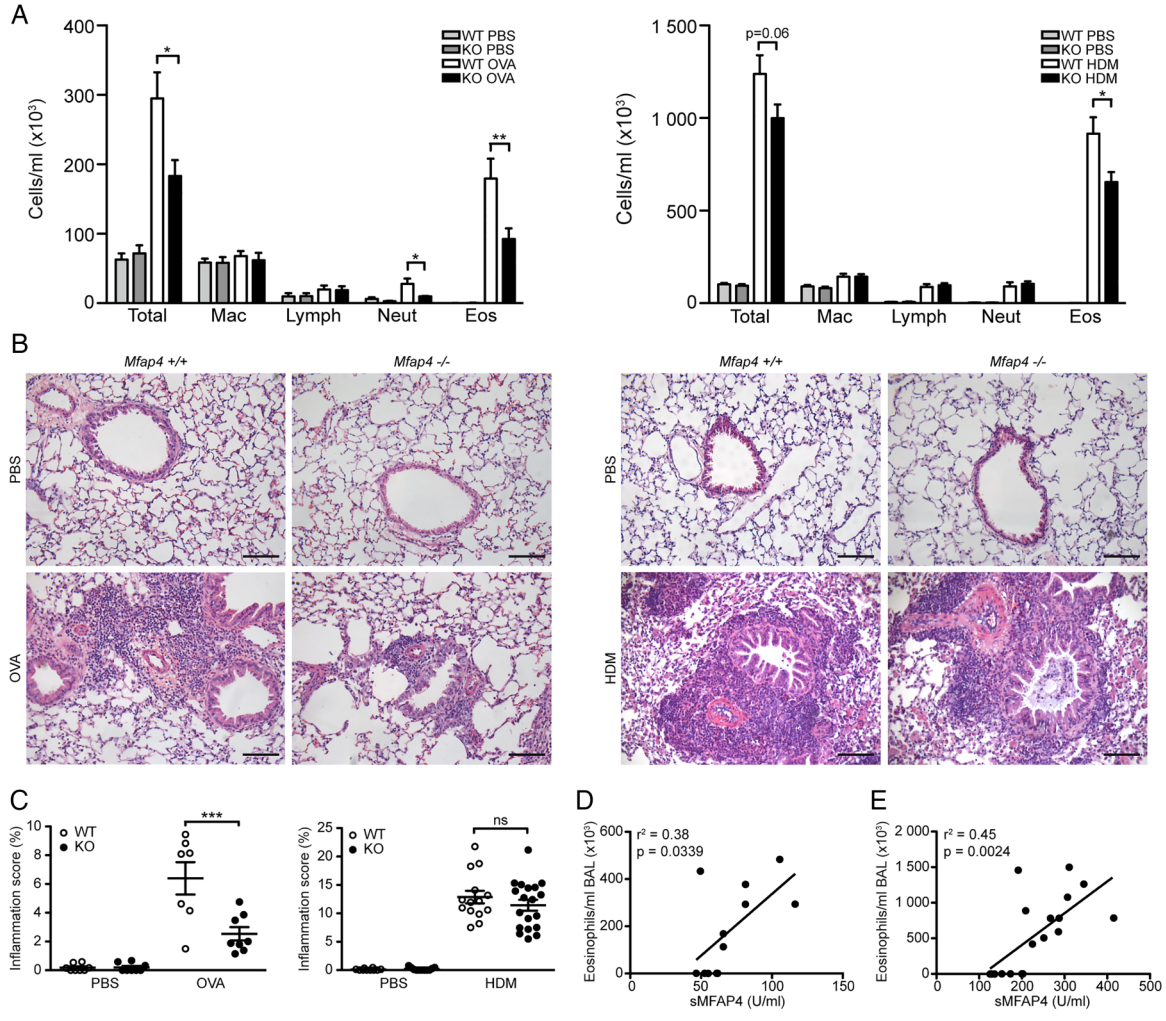

Figure 2 Microfibrillar-associated protein 4 (MFAP4) deficiency attenuates eosinophilic inflammation. (A) Both total cell count and eosinophil numbers in bronchoalveolar lavage (BAL) are lowered in MFAP4-deficient mice compared with wild-type (WT) littermates after ovalbumin (OVA) (left panel) or house dust mite (HDM) (right panel) treatment. (B) Representative pictures of H&E-stained lungs from OVA-treated (left panel) and HDM-treated (right panel) mice. (C) The degree of lung infiltration is lowered in MFAP4-deficient mice. Parenchymal inflammation was quantified in OVA-treated and HDM-treated animals. (D and E) Eosinophil counts in BAL correlated positively with MFAP4 concentration in serum of WT mice from (D) OVA and (E) HDM models. Scale bar, 100 µm. n=6 (OVA model), 10–11 (phosphate-buffered saline, PBS groups, HDM model), 14 (WT HDM), 19 (knockout, KO HDM). *p<0.05, **p<0.01, ***p<0.001, ns=not significant, calculated by one-way analysis of variance.

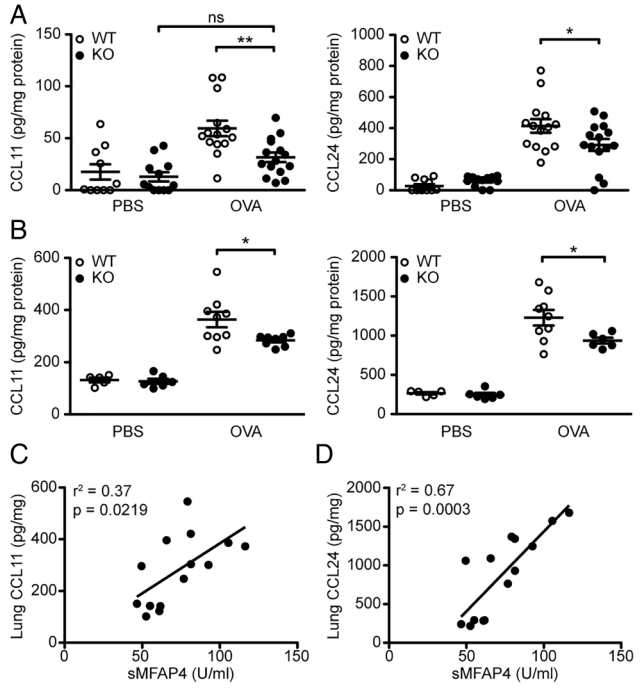

Figure 3 Microfibrillar-associated protein 4 (MFAP4) influences production of eotaxins. (A and B) Eotaxin-1 (CCL11) and eotaxin-2 (CCL24) were measured in (A) bronchoalveolar lavage (BAL) and (B) lung homogenate of ovalbumin (OVA)-treated mice. (C and D) Lung levels of both chemokines correlated positively with MFAP4 levels in serum of phosphate-buffered saline (PBS) and OVA treated wild-type (WT) mice. n=5–15. *p<0.05, **p<0.01, ns=not significant, calculated by one-way analysis of variance. KO, knockout.

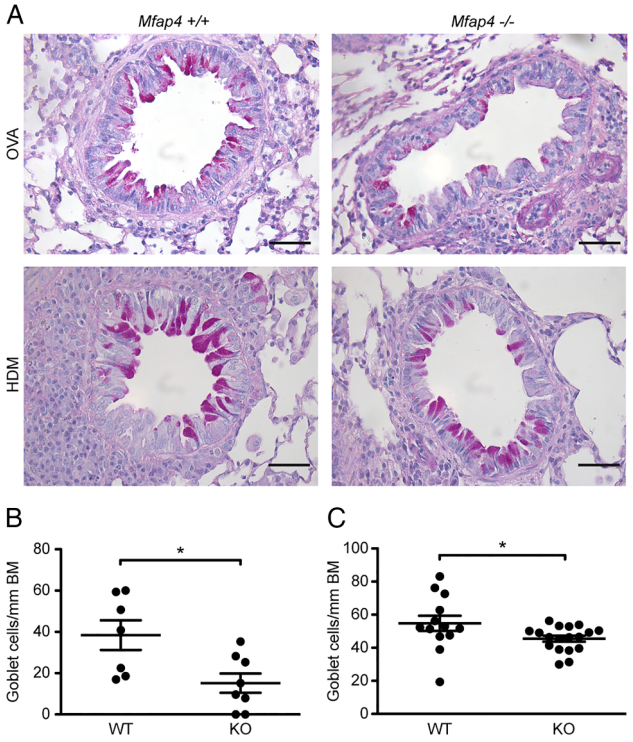

Figure 4 Microfibrillar-associated protein 4 (MFAP4) deficiency attenuates goblet cell metaplasia. (A) Representative pictures of periodic acid-Schiff (PAS)-stained lungs. (B and C) The degree of metaplasia was quantified in (B) ovalbumin (OVA)-treated and (C) house dust mite (HDM)-treated mice as the number of goblet cells normalised per length of the basement membrane (BM). Scale bar, 50 μm. n=7–19. *p<0.05, calculated by Student's t test. KO, knockout; WT, wild type.

resulted in downregulation of mucus production relative to WT mice, although to a smaller extent (figure 4C).

MFAP4-deficient mice are partially protected from ASM deposition and fibrosis

To investigate the influence of MFAP4 on airway remodelling, we performed morphometric analysis of ASM deposition and fibrotic changes (figure 5A, B). The increase in peribronchial smooth muscle layer thickness was absent or significantly reduced in MFAP4 KO mice (figure 5C). Moreover, HDM-treated MFAP4-deficient mice had significantly lowered total lung collagen content (figure 5D). Accordingly, the collagen-specific PSR-stained area was significantly diminished in treated MFAP4-deficient mice (figure 5E). OVA treatment did not influence hydroxyproline content or peribronchial collagen deposition (data not shown), suggesting that this acute challenge protocol has not induced significant airway remodelling other than ASM hyperplasia.

MFAP4 deficiency is protective against AHR

To specify the role of MFAP4 in AHR, we performed lung function analysis after MCh challenge. OVA exposure did not influence baseline resistance values, while chronic HDM treatment significantly increased baseline resistance independent of MFAP4 genotype (figure 6A). However, OVA-treated MFAP4-deficient mice demonstrated significantly lowered MCh-induced increase in pulmonary resistance than their WT littermates (figure 6B). The same tendency was observed in chronically treated animals (figure 6B). We then analysed data obtained from the so-called constant phase model, which divides resistance into central airway resistance of the conducting airways and tissue damping, a measure of resistance of lung parenchyma. We found that mainly changes in the parenchymal resistance are responsible for the overall attenuation of AHR in MFAP4-deficient mice (figure 6C, D).

MFAP4 is upregulated in asthmatic BSMCs

To further define the mechanism by which MFAP4 contributes to asthmatic airway disease, we studied the effects of MFAP4 on healthy or asthmatic human BSMCs in vitro. Using commercially available primary cells, we observed that asthmatic BSMCs produce increased levels of MFAP4 relative to BSMCs derived from the non-asthmatic donor, on mRNA (figure 7A) and protein level (figure 7B). We confirmed our initial observations on BSMCs isolated from a group of healthy subjects or patients with asthma, where we observed that mRNA and protein MFAP4 levels were clearly increased in the asthmatic group (figure 7C, D). The difference did not reach statistical significance, possibly due to large variation in the asthmatic group.

MFAP4 binds to BSMCs via integrin αvβ5 and activates FAK

We analysed expression of various integrin receptors on BSMC surface. We detected high levels of integrins β1 and αvβ5 and considerably lower levels of integrins β3 and αvβ3, whereas β6 and β8 subunits were undetected (see online supplementary figure S3). We then investigated the capacity and integrin dependence of MFAP4 to mediate BSMC adhesion. MFAP4 promoted adhesion of BSMCs in a dose-dependent manner, similarly in healthy and asthmatic cells (figure 8A) and to the level of the positive control

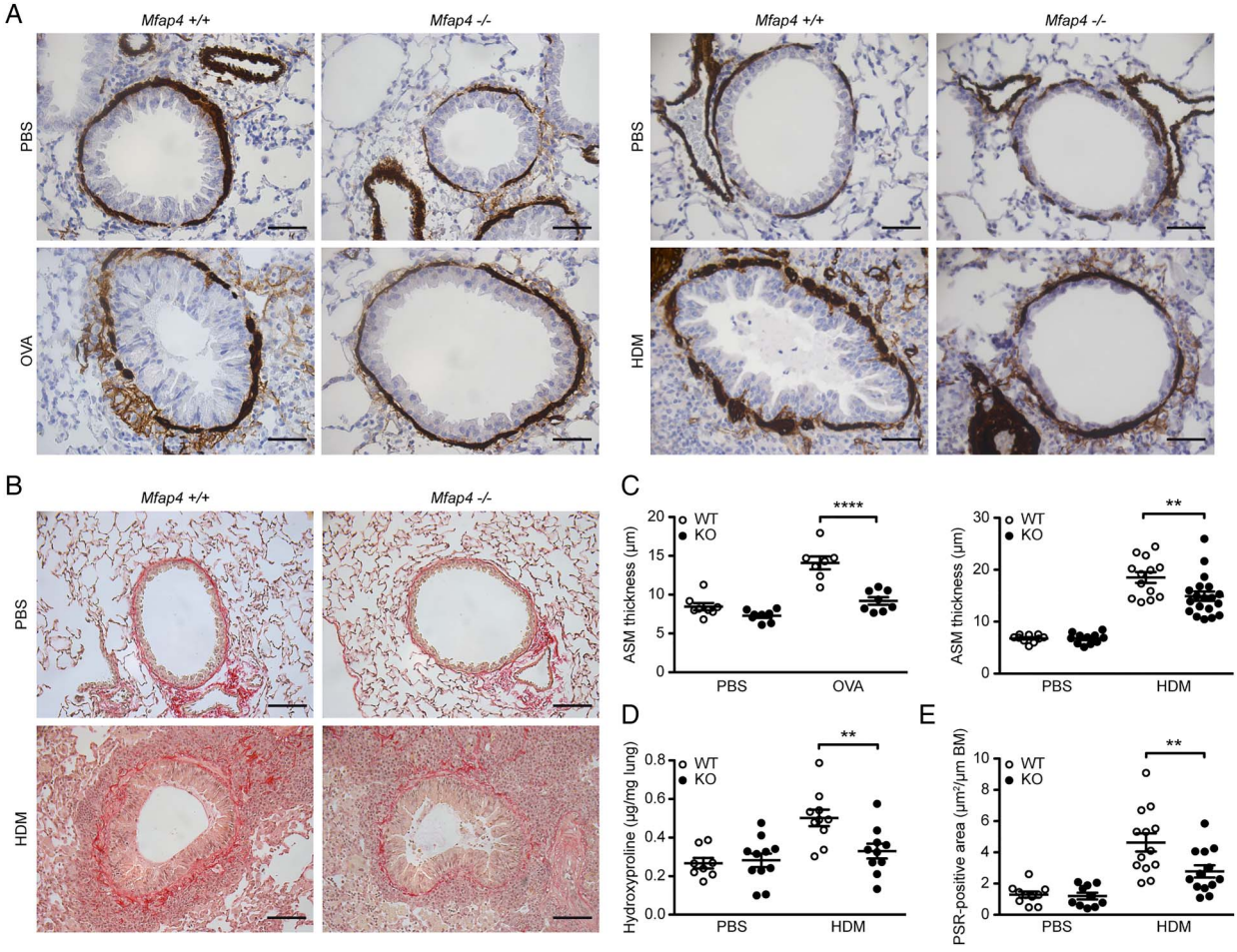

Figure 5 Microfibrillar-associated protein 4 (MFAP4) promotes bronchial smooth muscle cell remodelling and fibrosis. (A and B) Representative pictures of (A) α-smooth muscle actin (α-SMA)-stained and (B) Picrosirius Red (PSR)–stained lungs. (C) Smooth muscle deposition was quantified in ovalbumin (OVA)-treated and house dust mite (HDM)-treated mice as the thickness of peribronchial α-SMA-stained layer. (D–E) Both (D) total collagen lung content and (E) peribronchial collagen-stained area are lowered in MFAP4-deficient mice. ASM, airway smooth muscle. BM, basement membrane. Scale bar, 50 µm (A), 100 µm (B). n=7–19. **p<0.01, ****p<0.0001, calculated by one-way analysis of variance. ASM, airway smooth muscle; KO, knockout; PBS, phosphate-buffered saline; WT, wild type.

fibronectin (data not shown). MFAP4-dependent adhesion could be inhibited with a soluble RGD peptide but not with a control DGR peptide, suggesting that MFAP4 binds RGD-dependent integrins on BSMC surface (figure 8B, C). Moreover, anti-αv and anti-αvβ5 antibodies prohibited BSMC adhesion, showing that αvβ5 is the main MFAP4-binding partner on BSMCs (figure 8D). MFAP4 stimulation did not influence protein abundance of either integrin subunit (data not shown).

To verify if MFAP4 can promote initiation of cellular signalling, we checked time-dependent activation of FAK. Seeding healthy and asthmatic BSMCs on MFAP4 resulted in an increased time-dependent FAK phosphorylation relative to control cells seeded on poly-D-lysine (figure 8E).

MFAP4 promotes BSMC proliferation and CCL11 expression: role of αvβ5, PI3K and ERK1/2

We explored the influence of MFAP4 on the proliferative capacity of BSMCs. MFAP4 significantly increased BSMC proliferation in asthmatic BSMCs, while proliferation of healthy BSMCs was only slightly affected (figure 9A).

To further define signalling pathways involved in MFAP4-dependent BSMC proliferation, we cultured asthmatic BSMCs in the presence of anti-integrin antibodies or specific inhibitors of PI3K and MEK (MEK is an immediate upstream kinase crucial for ERK1/2 activation). We found that MFAP4-mediated proliferation was inhibited by anti-integrin αvβ5 blocking antibody (figure 9B). Moreover, MFAP4-dependent proliferation was inhibited dose-dependently by PI3K inhibitor but not by MEK inhibitor (figure 9C, D).

Finally, we investigated if MFAP4 influences pro-asthmatic secretory properties of BSMCs. As expected, mRNA expression of CCL11 was strongly enhanced in asthmatic BSMCs compared with healthy cells. Furthermore, CCL11 expression was upregulated in asthmatic BSMCs seeded on MFAP4 compared with cells seeded on control coating (figure 9E). MFAP4-dependent increase in CCL11 expression was inhibited by PI3K but not MEK inhibitor (figure 9F, G).

DISCUSSION

In the present study, we evaluated the role of MFAP4 in OVA-mediated and HDM-mediated allergic asthma models. We showed that OVA and HDM treatments result in elevated serum MFAP4. We further demonstrated that antigen-challenged MFAP4-deficient mice exhibit reduced eosinophilia, goblet cell metaplasia, ASM deposition and AHR compared with WT mice, whereas IgE responses and IL-4 and IL-5 levels remain

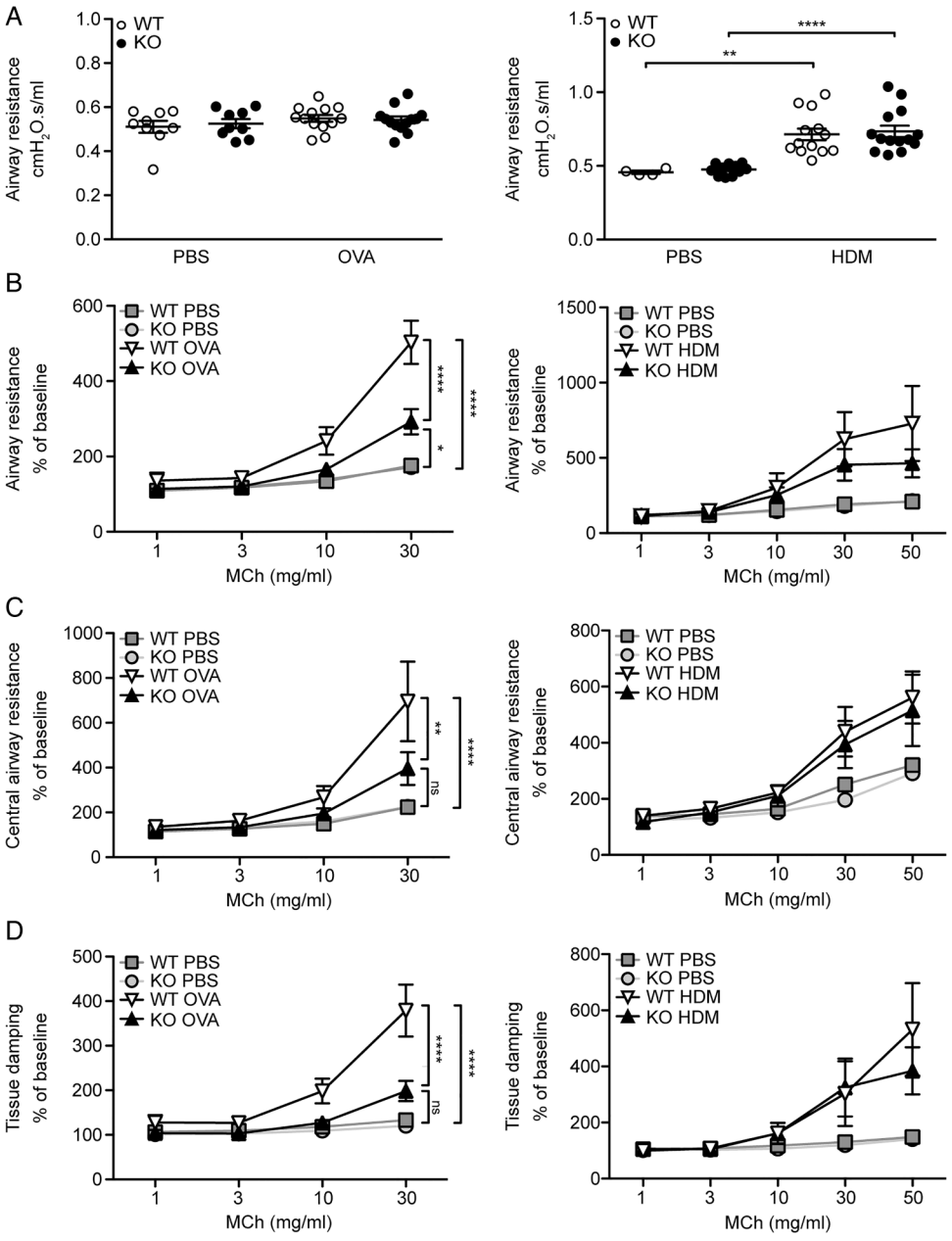

Figure 6 Microfibrillar-associated protein 4 (MFAP4) deficiency reduces airway hyperresponsiveness in ovalbumin (OVA)-treated but not house dust mite (HDM)-treated mice. (A) Basal airway resistance after OVA (left) or HDM (right) exposure. (B–D) Airway reactivity to increased doses of methacholine (MCh), measured as increase in (B) resistance, (C) central airway resistance and (D) tissue damping was strongly attenuated in OVA-treated MFAP4-deficient mice (left) but only slightly lowered in HDM-treated MFAP4-deficient mice (right). n=5–8 (OVA model), 5–13 (HDM model). *p<0.05, **p<0.01, ****p<0.0001, ns=not significant, calculated by two-way analysis of variance. KO, knockout; PBS, phosphate-buffered saline; WT, wild type.

unchanged. We also showed that MFAP4 is upregulated in asthmatic BSMCs, and that it promotes BSMC integrin-dependent adhesion, proliferation and CCL11 release. Collectively, we suggest MFAP4 as an important contributor to allergic asthma.

MFAP4 levels were increased in serum in OVA-treated mice and in serum and BAL in HDM-treated mice but were decreased in lung homogenates. This suggests that MFAP4 is released to the circulation due to increased matrix turnover and remodelling accompanying disease progression. Elevated MFAP4 expression in asthmatic BSMCs indicates that increased local MFAP4 production may contribute to elevated levels of circulating MFAP4. We showed that MFAP4 is upregulated in asthmatic BSMCs, but other mesenchymal cell types such as vascular SMCs or fibroblasts may constitute another potential source of serum MFAP4. However, this possibility was not explored further.

Correlations between serum MFAP4 and eosinophil numbers and eosinophil chemoattractants support a functional link between MFAP4 and allergic airway disease. Studies that aim to translate this observation by testing serum MFAP4 variation in patients with asthma are thus warranted, in order to assess if MFAP4 may serve as a predictor of eosinophilic asthma in humans.

Eotaxins are potent chemokines playing a crucial role in eosinophil accumulation in asthmatic airways.[16] Disturbing eotaxins or their receptor CCR3 impaired lung eosinophil

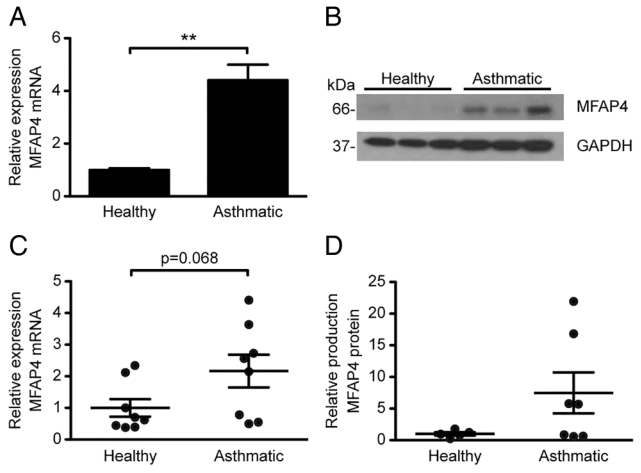

Figure 7 Microfibrillar-associated protein 4 (MFAP4) is upregulated in asthmatic bronchial smooth muscle cells (BSMCs). MFAP4 mRNA expression (A and C) and protein production (B and D) is increased in commercially available asthmatic BSMCs (A and B) as well as BSMCs isolated from patients with asthma (C and D) relative to healthy BSMCs. Data are means+SEM (A) or representative (B) of three independent experiments. n=5–8 (C and D). **p<0.01, calculated by Student's t test.

recruitment after antigen challenge, which was accompanied in most, but not all, studies by a decrease in goblet cell metaplasia and AHR.[17 18] We found reduced levels of eotaxins in the lungs of OVA-treated MFAP4-deficient mice. BSMCs have been previously shown to upregulate CCL11 and other eosinophil-related chemoattractants after stimulation with ECM.[19] Our results indicate that MFAP4 contributes to antigen-induced eosinophilia primarily through BSMC-derived CCL11, and can thus indirectly affect goblet cell metaplasia and AHR. However, eotaxins can also be abundantly produced by alveolar macrophages and epithelial cells.[20] It is then possible that MFAP4 deficiency results in lowered antigen-induced production of these chemokines from other cell types.

Epithelial transdifferentiation towards mucus-producing cells is strongly influenced by IL-13.[21] We found that MFAP4 deficiency resulted in attenuation of goblet cell hyperplasia together with a decrease in local IL-13. However, BSMCs in our in vitro setting did not produce significant amounts of IL-13 (data not shown). We did not investigate MFAP4 effects on other cell types, but both epithelial cells and alveolar macrophages may be relevant sources of IL-13.[22 23] Considering their expression of RGD-dependent integrins, it is conceivable that MFAP4 may directly regulate IL-13 secretion in these cells. Further studies are needed to clarify these issues.

ASM proliferation is one of the most important causes of airway narrowing and AHR.[24] We found that BSMC proliferation was directly influenced by MFAP4, and that lack of MFAP4 partially normalised peribronchial ASM thickness and consequently AHR. Moreover, MFAP4 may also contribute to increased BSMC deposition through eosinophil-dependent hyperplasia.[25]

Although OVA-induced AHR was strongly attenuated in KO mice, we detected only a tendency towards decreased airway resistance in HDM-treated KO mice. It is possible that severe inflammation after 7-week HDM exposure masked the effects of MFAP4 deficiency on AHR. The two models are mechanistically different; OVA sensitisation together with alum adjuvant with subsequent challenge elicits strong Th2-based adaptive

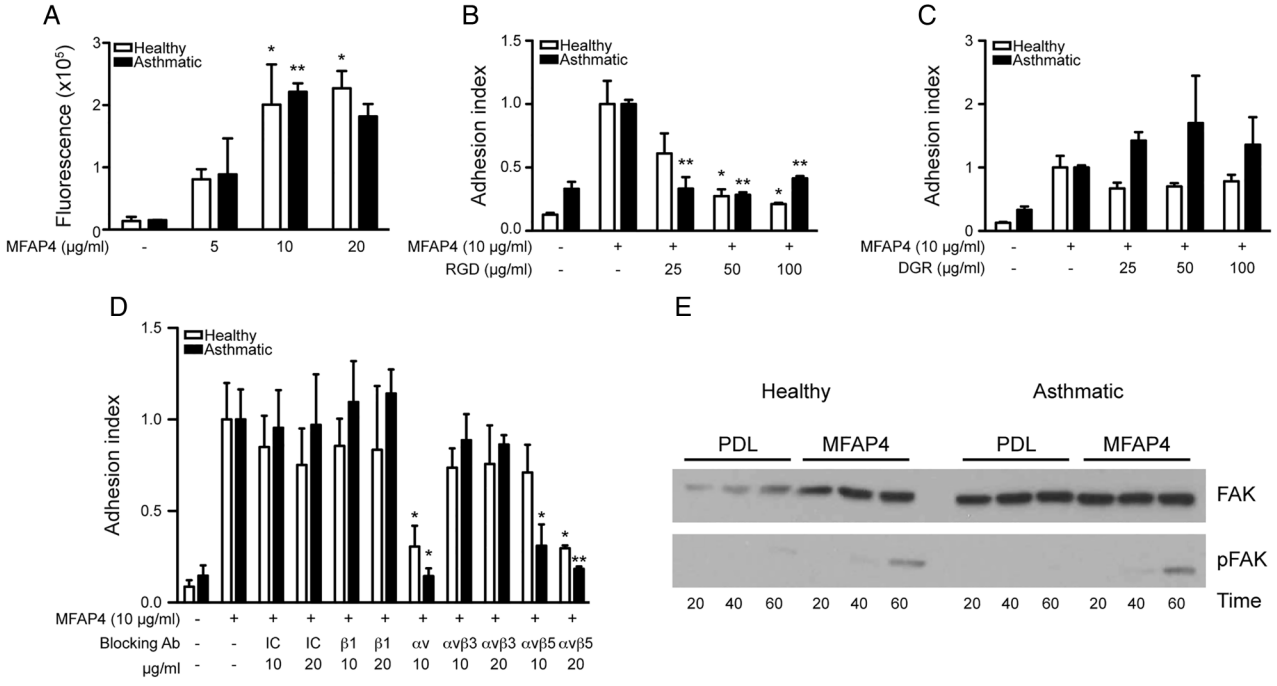

Figure 8 Microfibrillar-associated protein 4 (MFAP4) promotes bronchial smooth muscle cell (BSMC) attachment through integrin αvβ5 and focal adhesion kinase (FAK) activation. (A) MFAP4 promotes BSMC adhesion in a dose-dependent manner. (B and C) MFAP4-dependent adhesion can be inhibited by (B) RGD blocking peptide but not (C) DGR control peptide. (D) BSMC adhesion to MFAP4 is inhibited by integrin αvβ5-blocking antibodies. (E) Western blot analysis shows FAK phosphorylation after seeding cells on MFAP4. Data are means+SEM (A–D) or representative (E) of at least three independent experiments. *p<0.05, **p<0.01 compared with relevant uncoated (A), MFAP4-coated (B and C) or IC control (D), calculated by one-way analysis of variance. IC, isotype control; PDL, poly-D-lysine.

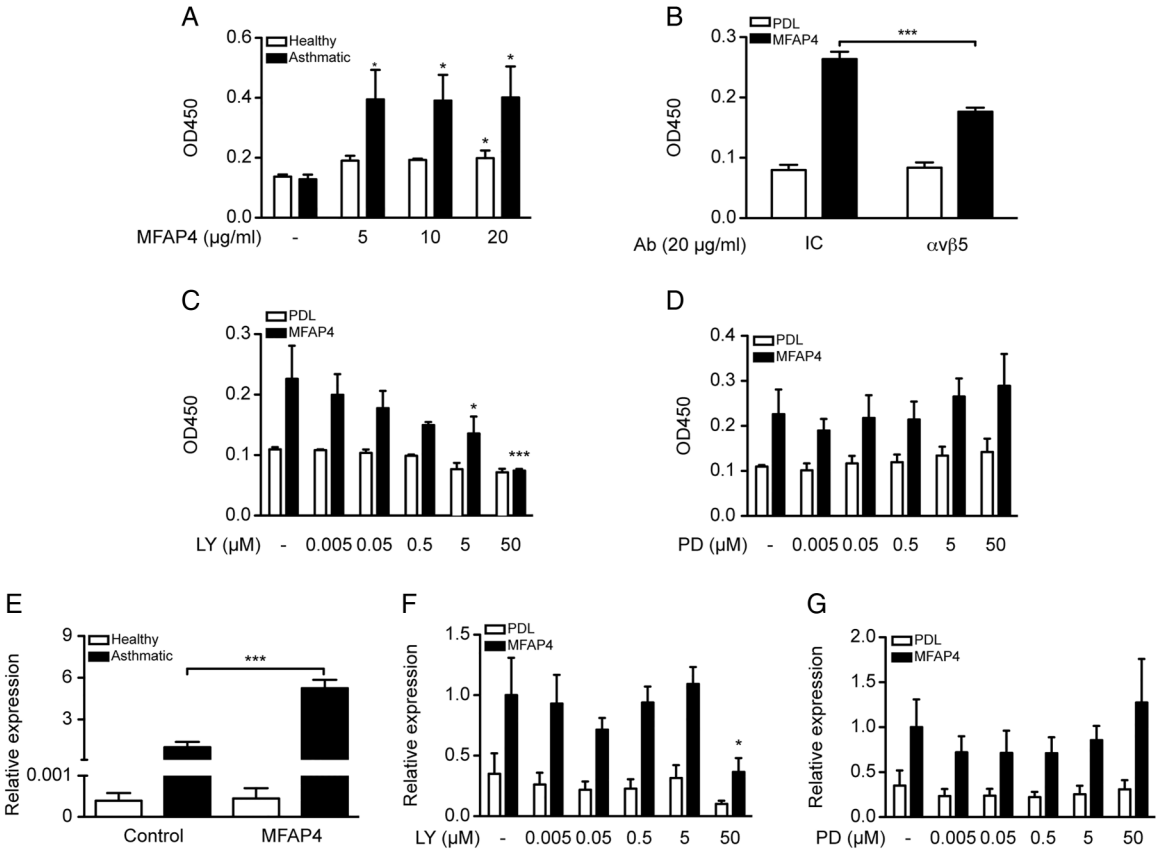

Figure 9 Microfibrillar-associated protein 4 (MFAP4) promotes asthmatic bronchial smooth muscle cell (BSMC) proliferation and CCL11 expression through integrin αvβ5 and PI3K. (A) MFAP4 enhances asthmatic BSMC proliferation. (B) MFAP4-dependent asthmatic BSMC proliferation can be inhibited by integrin αvβ5-blocking antibody. (C and D) MFAP4-dependent asthmatic BSMC proliferation is blocked by PI3K inhibitor (C) but not MEK inhibitor (D). (E) MFAP4 enhances CCL11 mRNA expression in asthmatic BSMCs. Asthmatic cells seeded on MFAP4 (MFAP4, right) express higher levels of CCL11 than cells seeded on vehicle coating (control, left). (F and G) MFAP4-dependent CCL11 upregulation is inhibited by PI3K inhibitor (F) but not MEK inhibitor (G). DMSO was used as a vehicle control for kinase inhibitors. Data are means+SEM of at least three independent experiments. *p<0.05, **p<0.01, ***p<0.001 compared with relevant coating control, calculated by one-way analysis of variance. IC, isotype control; LY, LY294002; OD, optical density; PD, PD98059; PDL, poly-D-lysine.

response that is dependent on $CD4^+$ T cells, while repeated local exposure to protease-containing HDM induces more innate response.[26] Moreover, even for the same allergen, pathophysiological mechanisms might depend on the duration of the model, as shown for STAT6 involvement in AHR development evident in the acute but not chronic model of OVA exposure (reviewed in[27]). This underlines that mechanisms driving AHR might be context specific.

We assessed the contributions of central airways and lung parenchyma to the overall AHR increase. The main effect was mediated through changes in tissue damping, a parameter reflecting parenchymal resistance. As the increase in tissue damping is a manifestation of small airway constriction,[28] the data suggest that MFAP4-related effects on AHR are caused by inflammation and remodelling in the parenchyma.

There is limited knowledge on expression of integrin receptors on BSMCs. In several studies, α5, αv and β1 subunits were found to be universally expressed, together with moderate expression of α1–α8 and low levels of β3.[29] They serve as recognition partners for ECM components such as fibronectin, an established inducer of BSMC proliferation.[2] In agreement with existing literature, our data show that BSMCs express high levels of integrin β1 and low levels of integrin β3. We also found high expression of integrin αvβ5 heterodimer, and showed that it serves as a recognition partner for MFAP4. αvβ5 was previously found to activate TGF-β and promote airway remodelling.[30] Furthermore, a recent genome-wide study identified ITGB5, a gene coding for integrin β5, to be strongly associated to AHR severity in patients with asthma.[31] Our results showed that MFAP4-mediated proliferation was αvβ5-dependent, and thus suggest that interactions between αvβ5 and its ligands, such as MFAP4, contribute to excessive BSMC proliferation seen in asthma.

We detected changes in FAK activation shortly after plating cells onto MFAP4, suggesting that FAK is directly activated by MFAP4-binding integrins. To our knowledge, only one study so far addressed the role of FAK in integrin signalling in ASM, showing that FAK promotes collagen I induced bovine ASM proliferation together with activation of PI3K and ERK.[32] Both these pathways regulate growth factor-induced ASM growth, though PI3K seems to be more important in asthmatic ASM.[33] Moreover, PI3 signalling has been previously implicated in the regulation of CCL11 expression in ASM, and pharmacological PI3K inhibition has been shown to protect from OVA-induced asthma.[34] We demonstrated that MFAP4 effects on proliferation and CCL11 release were inhibited by PI3K but not by ERK pathway blockage, thus identifying a possible mechanism underlying MFAP4-mediated effects.

Integrin signalling and downstream PI3K activation has been shown to promote AP-1 and NF-κB-dependent gene expression (reviewed in Guo and Giancotti[35]). Binding sites for both these

transcription factors lie within the CCL11 promoter region,[36] which makes them plausible candidates for mediating MFAP4-related CCL11 upregulation.

Isolated human BSMCs are known to retain their phenotype in vitro, and the phenotypic difference between healthy and asthmatic BSMCs is conserved during isolation and culture. One possible reason might be abnormal calcium homeostasis in asthmatic BSMCs, which is unchanged even after several passages.[37]

Our study contains several limitations. Human asthma is a complex, heterogeneous disease, manifesting itself in a variety of endotypes.[38] The animal models used suggest that MFAP4 contributes to canonical, eosinophilic asthma, but on the basis of the current study we cannot address the possible role of MFAP4 in other subphenotypes, such as neutrophil-rich asthma. Moreover, as our in vitro assays were performed on cells obtained from one donor pair only, they do not provide a full understanding of MFAP4 impact on BSMC behaviour. Further studies, including detailed analysis of patient-derived cells, are thus of interest.

In conclusion, our data indicate that MFAP4 contributes to allergic asthma by promoting airway eosinophilia, AHR and lung remodelling through regulation of ASM proliferation and eotaxin secretion. Our characterisation of this novel pathway involved in asthma pathogenesis might open new research avenues focused on future development of new therapeutic strategies.

Author affiliations
[1]Institute of Molecular Medicine, University of Southern Denmark, Odense, Denmark
[2]Department of Pharmacology, Bordeaux University, Cardio-thoracic Research Centre, U1045, Bordeaux, France
[3]Department of Pathology, Odense University Hospital, Odense, Denmark
[4]German Research Center for Environmental Health, German Mouse Clinic and Institute of Experimental Genetics, Helmholtz Zentrum Munich, Neuherberg, Germany
[5]Department of Dermatology and Allergology am Biederstein, University Hospital Klinikum rechts der Isar, Technical University Munich, Munich, Germany
[6]Chair of Experimental Genetics, Center of Life and Food Sciences Weihenstephan, Technical University Munich, Freising-Weihenstephan, Germany
[7]Department of Respiratory Medicine, Gentofte Hospital, Hellerup, Denmark
[8]Manchester Academic Health Science Centre, University Hospital South Manchester NHS Foundation Trust, Manchester, UK
[9]Department of Lung Function Testing, Department of Thoracic Chirurgy, Department of Anatomy and Pathology, CHU Bordeaux Teaching Hospital, Pessac, France

Acknowledgements We thank Vicki Nielsen, Charlotte Skouboe Landré and Ida Tornoe (Institute of Molecular Medicine, Odense, Denmark) for excellent technical assistance. We also thank Christopher Stevenson (Novartis, Horsham, UK) for providing HDM extract and valuable advice.

Contributors BP performed experiments, analysed data and wrote the manuscript; AS, HWJ, TT, JBM, NM, JAAP, MHDA, PB participated in data collection and analysis; JV, UH participated in study conception; JBM, JV, UH, GLS, reviewed the manuscript; GLS conceived and supervised the study. BP and GLS are the guarantors responsible for the overall content of the manuscript.

Funding This work was supported by the Lundbeck Foundation, Region of Southern Denmark, Fonden til Laegevidenskabens Fremme, Direktor Jacob Madsen og hustru Olga Madsens Fond, Aase og Ejnar Danielsens Fond, Linexfonden, the Danish Strategic Research Council (the Centre of COPD Research, http://www.cekol.dk) (09-066945) and German Federal Ministry of Education and Research (Infrafrontier grant 01KX1012).

Competing interests AS, UH and GLS have issued a patent: MFAP4 binding antibodies blocking the interaction between MFAP4 and integrin receptors: P1183DK00. JV has not received any financial support in relation to the current manuscript. Outside this work he has received honoraria for advising and presenting from AstraZeneca, Boehringer-Ingelheim, Chiesi, GSK, and Novartis.

Ethics approval Local ethics committee at the Bordeaux Teaching Hospital.

Provenance and peer review Not commissioned; externally peer reviewed.

REFERENCES

1 Woodruff PG, Dolganov GM, Ferrando RE, *et al*. Hyperplasia of smooth muscle in mild to moderate asthma without changes in cell size or gene expression. *Am J Respir Crit Care Med* 2004;169:1001–6.
2 Nguyen TT, Ward JP, Hirst SJ. beta1-Integrins mediate enhancement of airway smooth muscle proliferation by collagen and fibronectin. *Am J Respir Crit Care Med* 2005;171:217–23.
3 Johnson PR, Burgess JK, Underwood PA, *et al*. Extracellular matrix proteins modulate asthmatic airway smooth muscle cell proliferation via an autocrine mechanism. *J Allergy Clin Immunol* 2004;113:690–6.
4 Peng Q, Lai D, Nguyen TT, *et al*. Multiple beta 1 integrins mediate enhancement of human airway smooth muscle cytokine secretion by fibronectin and type I collagen. *J Immunol* 2005;174:2258–64.
5 Dekkers BG, Bos IS, Gosens R, *et al*. The integrin-blocking peptide RGDS inhibits airway smooth muscle remodeling in a guinea pig model of allergic asthma. *Am J Respir Crit Care Med* 2010;181:556–65.
6 Giancotti FG, Ruoslahti E. Integrin signaling. *Science* 1999;285:1028–32.
7 Wulf-Johansson H, Lock Johansson S, Schlosser A, *et al*. Localization of microfibrillar-associated protein 4 (MFAP4) in human tissues: clinical evaluation of serum MFAP4 and its association with various cardiovascular conditions. *PLoS ONE* 2013;8:e82243.
8 Toyoshima T, Nishi N, Kusama H, *et al*. 36-kDa microfibril-associated glycoprotein (MAGP-36) is an elastin-binding protein increased in chick aortae during development and growth. *Exp Cell Res* 2005;307:224–30.
9 Kasamatsu S, Hachiya A, Fujimura T, *et al*. Essential role of microfibrillar-associated protein 4 in human cutaneous homeostasis and in its photoprotection. *Sci Rep* 2011;1:164.
10 Johansson SL, Roberts NB, Schlosser A, *et al*. Microfibrillar-associated protein 4: a potential biomarker of chronic obstructive pulmonary disease. *Respir Med* 2014;108:1336–44.
11 Brandsma CA, van den Berge M, Postma DS, *et al*. A large lung gene expression study identifying fibulin-5 as a novel player in tissue repair in COPD. *Thorax* 2015;70:21–32.
12 Holm AT, Wulf-Johannson H, Hvidsten S, *et al*. Characterization of spontaneous airspace enlargement in mice lacking microfibrillar-associated protein 4. *Am J Physiol Lung Cell Mol Physiol* 2015;308:L1114–24.
13 Gregory LG, Causton B, Murdoch JR, *et al*. Inhaled house dust mite induces pulmonary T helper 2 cytokine production. *Clin Exp Allergy* 2009;39:1597–610.
14 (GINA). Global Initiative for Asthma. Global strategy for asthma management and prevention. NIH Publication (updated 2014). 1995. http://www.ginasthma.org
15 Trian T, Allard B, Dupin I, *et al*. House dust mites induce proliferation of severe asthmatic smooth muscle cells via an epithelium-dependent pathway. *Am J Respir Crit Care Med* 2015;191:538–46.
16 Lilly CM, Nakamura H, Belostotsky OI, *et al*. Eotaxin expression after segmental allergen challenge in subjects with atopic asthma. *Am J Respir Crit Care Med* 2001;163:1669–75.
17 Fulkerson PC, Fischetti CA, McBride ML, *et al*. A central regulatory role for eosinophils and the eotaxin/CCR3 axis in chronic experimental allergic airway inflammation. *Proc Natl Acad Sci USA* 2006;103:16418–23.
18 Wegmann M, Goggel R, Sel S, *et al*. Effects of a low-molecular-weight CCR-3 antagonist on chronic experimental asthma. *Am J Respir Cell Mol Biol* 2007;36:61–7.
19 Chan V, Burgess JK, Ratoff JC, *et al*. Extracellular matrix regulates enhanced eotaxin expression in asthmatic airway smooth muscle cells. *Am J Respir Crit Care Med* 2006;174:379–85.
20 Ying S, Meng Q, Zeibecoglou K, *et al*. Eosinophil chemotactic chemokines (eotaxin, eotaxin-2, RANTES, monocyte chemoattractant protein-3 (MCP-3), and MCP-4), and C-C chemokine receptor 3 expression in bronchial biopsies from atopic and nonatopic (Intrinsic) asthmatics. *J Immunol* 1999;163:6321–9.
21 Leigh R, Ellis R, Wattie J, *et al*. Is interleukin-13 critical in maintaining airway hyperresponsiveness in allergen-challenged mice? *Am J Respir Crit Care Med* 2004;170:851–6.
22 Semlali A, Jacques E, Koussih L, *et al*. Thymic stromal lymphopoietin-induced human asthmatic airway epithelial cell proliferation through an IL-13-dependent pathway. *J Allergy Clin Immunol* 2010;125:844–50.
23 Prieto J, Lensmar C, Roquet A, *et al*. Increased interleukin-13 mRNA expression in bronchoalveolar lavage cells of atopic patients with mild asthma after repeated low-dose allergen provocations. *Respir Med* 2000;94:806–14.
24 Boulet LP, Turcotte H, Laviolette M, *et al*. Airway hyperresponsiveness, inflammation, and subepithelial collagen deposition in recently diagnosed versus long-standing mild asthma. Influence of inhaled corticosteroids. *Am J Respir Crit Care Med* 2000;162(4 Pt 1):1308–13.
25 Halwani R, Vazquez-Tello A, Sumi Y, *et al*. Eosinophils induce airway smooth muscle cell proliferation. *J Clin Immunol* 2013;33:595–604.
26 Boyce JA, Austen KF. No audible wheezing: nuggets and conundrums from mouse asthma models. *J Exp Med* 2005;201:1869–73.

27 Kumar RK, Herbert C, Foster PS. The 'classical' ovalbumin challenge model of asthma in mice. *Curr Drug Targets* 2008;9:485–94.
28 Pinelli V, Marchica CL, Ludwig MS. Allergen-induced asthma in C57Bl/6 mice: hyper-responsiveness, inflammation and remodelling. *Respir Physiol Neurobiol* 2009;169:36–43.
29 Freyer AM, Johnson SR, Hall IP. Effects of growth factors and extracellular matrix on survival of human airway smooth muscle cells. *Am J Respir Cell Mol Biol* 2001;25:569–76.
30 Tatler AL, John AE, Jolly L, *et al*. Integrin alphavbeta5-mediated TGF-beta activation by airway smooth muscle cells in asthma. *J Immunol* 2011;187:6094–107.
31 Himes BE, Qiu W, Klanderman B, *et al*. ITGB5 and AGFG1 variants are associated with severity of airway responsiveness. *BMC Med Genet* 2013;14:86.
32 Dekkers BG, Spanjer AI, van der Schuyt RD, *et al*. Focal adhesion kinase regulates collagen I-induced airway smooth muscle phenotype switching. *J Pharmacol Exp Ther* 2013;346:86–95.
33 Burgess JK, Lee JH, Ge Q, *et al*. Dual ERK and phosphatidylinositol 3-kinase pathways control airway smooth muscle proliferation: differences in asthma. *J Cell Physiol* 2008;216:673–9.
34 Duan W, Aguinaldo Datiles AM, Leung BP, *et al*. An anti-inflammatory role for a phosphoinositide 3-kinase inhibitor LY294002 in a mouse asthma model. *Int Immunopharmacol* 2005;5:495–502.
35 Guo W, Giancotti FG. Integrin signalling during tumour progression. *Nat Rev Mol Cell Biol* 2004;5:816–26.
36 Nie M, Knox AJ, Pang L. beta2-Adrenoceptor agonists, like glucocorticoids, repress eotaxin gene transcription by selective inhibition of histone H4 acetylation. *J Immunol* 2005;175:478–86.
37 Mahn K, Hirst SJ, Ying S, *et al*. Diminished sarco/endoplasmic reticulum Ca2+ ATPase (SERCA) expression contributes to airway remodelling in bronchial asthma. *Proc Natl Acad Sci USA* 2009;106:10775–80.
38 Anderson GP. Endotyping asthma: new insights into key pathogenic mechanisms in a complex, heterogeneous disease. *Lancet* 2008;372:1107–19.

Microfibrillar-associated protein 4 modulates airway smooth muscle cell phenotype in experimental asthma

Bartosz Pilecki[1], Anders Schlosser[1], Helle Wulf-Johansson[1], Thomas Trian[2], Jesper B. Moeller[1], Niels Marcussen[3], Juan Antonio Aguilar-Pimentel[4,5], Martin Hrabě de Angelis[4,6], Jørgen Vestbo[7,8], Patrick Berger[2,9], Uffe Holmskov[1], Grith L. Sorensen[1]

SUPPLEMENTARY MATERIAL

Source of reagents

HDM was from Greer (Lenoir, NC, USA). Alum was from Thermo Scientific (Waltham, MA, USA). CCL11 ELISA kit, CCL24 ELISA kit and recombinant human PDGF-BB were from R&D (Minneapolis, MN, USA). IL4 ELISA kit was from Biolegend (San Diego, CA, USA). IL5 ELISA kit and IL13 ELISA kit were from eBioscience (San Diego, CA, USA). Anti-IgE-HRP antibody was from Southern Biotech (Birmingham, AL, USA). Rabbit anti-FITC antibody, goat anti-rabbit Ig-HRP antibody and DAB+ chromogen were from Dako (Glostrup, Denmark). Hydroxyproline Colorimetric Assay Kit was from Biovision (Milpitas, CA, USA). TRIzol and amphotericin B reagent were from Invitrogen (Waltham, MA, USA). NucleoSpin RNA kit was from Macherey-Nagel (Hoerdt, France). Hemacolor staining kit, anti-integrin αvβ3 antibody and anti-integrin β1 antibody were from Millipore (Billerica, MA, USA). Anti-integrin αv antibody was from Alexis Biochemicals (Enzo Life Sciences, Farmingdale, NY, USA). Protease and phosphatase inhibitors were from Roche (Basel, Switzerland). Pre-cast SDS-PAGE gels and nonfat dry milk were from Biorad (Hercules, CA, USA). ECL detection reagents were from Amersham (GE Healthcare, Chalfont St. Giles, UK). BSMCs were obtained from Lonza (Basel, Switzerland). DMEM, FBS, antibiotics and L-glutamine were obtained from Gibco (Waltham, MA, USA). Alfazyme was from PAA Laboratories (GE Healthcare, Chalfont St. Giles, UK). Vybrant Cell Adhesion Assay Kit was from Molecular Probes (Waltham, MA, USA). Anti-GAPDH antibody and anti-αvβ5 antibody were from Santa Cruz (Dallas, TX, USA). BrdU Cell Proliferation Assay Kit, anti-FAK antibody, anti-pFAK(T397) antibody, anti-integrin β5 antibody, PI3K inhibitor and MEK inhibitor were from Cell Signaling Technology (Danvers, MA, USA). Anti-MFAP4 monoclonal antibodies were produced in our laboratory. All other reagents were obtained from Sigma-Aldrich (St. Louis, MO, USA).

Measurement of lung mechanics and AHR

24 h after the last challenge mice were anesthetized intraperitoneally with ketamine (100 mg/kg) and xylazine (10 mg/kg), tracheostomized and connected to computer-controlled small animal ventilator (Flexivent, SCIREQ, Montreal, Canada). Mechanical ventilation was set at 150 breaths/min with a tidal volume of 10 ml/kg and a positive end-expiratory pressure of 3 cm H_2O. Lung function parameters were measured in the steady state and after exposure to increasing doses of nebulized methacholine (MCh). For each parameter, a coefficient of determination of 0.90 was the lower limit for accepting a measurement.

Bronchoalveolar lavage (BAL)

Immediately after AHR measurements mice were sacrificed by cardiac puncture. Lungs were washed four times with 0.5 ml ice-cold PBS. BAL fluids were centrifuged at 1,000 g for 10 min at 4°C, and supernatants were stored in -80°C until further analysis. Cells were washed in red blood cell lysis buffer, resuspended in PBS, counted, cytospun and stained with Hemacolor. Differential cell count was performed in a blinded manner by two independent observers.

Preparation of lung homogenates

Frozen lungs were homogenized in 1 ml PBS with protease inhibitors. Homogenates were centrifuged for 10,000 g at 4°C. The supernatants were stored in -80°C until further analysis.

Measurement of specific IgE

Specific IgE was measured by ELISA. Briefly, wells were coated with 5 μg/ml OVA or HDM overnight at 4°C. Wells were blocked with PBS/0,05% Tween/1% BSA for 1 h. Serum samples diluted 1:20 in blocking buffer were then incubated for 2 h, after which wells were

washed and incubated with anti-IgE-HRP antibody. Results are shown as relative absorbance units (OD450).

Lung histology

Formalin-fixed, paraffin-embedded lung tissues were cut in 4 μm-thick slides and stained with hematoxylin and eosin (H&E), periodic acid-Schiff (PAS), or Picrosirius Red (PSR). For immunohistochemistry, sections were subjected to antigen retrieval with 1.5% hydrogen peroxide, stained with FITC-conjugated antibodies against α-smooth muscle actin (α-SMA) or MFAP4 (dilution 1:1000 and 1:100, respectively) for 1 h and secondary rabbit anti-FITC antibody for 20 min, and visualized with goat anti-rabbit Ig-HRP antibody and DAB+ chromogen.

Morphometric analysis

Lung inflammation was graded on H&E-stained slides by point counting using CAST 1 software. Briefly, 36-point grid was laid onto the field of vision. In each of 25 randomly selected fields, points hitting the inflamed area as well as all points hitting lung parenchyma were counted. The degree of inflammation was quantified as the ratio between the number of points hitting the inflamed area and the total number of points, and is presented as percentage of inflamed lung area.

Subepithelial fibrosis was quantified by color threshold analysis as Picrosirius Red-positive area and normalized to the length of the basement membrane. Goblet cell hyperplasia was assessed by counting PAS-positive cells and normalizing to the length of the basement membrane. Smooth muscle cell remodeling was quantified by measuring the thickness of the smooth muscle cell layer around airways. At least 5 same-sized bronchioles were counted in each slide. All analyses were performed in a blinded manner using ImageJ software [S1].

Cytokine quantifications

The levels of IL-4, IL-5, IL-13, CCL11 and CCL24 in BAL or lung homogenates were measured using commercial ELISA kits according to the manufacturers' instructions. The minimum detection limits were: 1 pg/ml for IL-4, 4 pg/ml for IL-5 and IL-13, and 3 pg/ml for CCL11 and CCL24.

Hydroxyproline assay

Levels of hydroxyproline in lung tissues, being a surrogate for collagen content, were measured using Hydroxyproline Colorimetric Assay Kit according to the manufacturer's instructions.

Surface coating with ECM proteins

Tissue culture plates were left uncoated or incubated with 5-20 µg/ml of poly-D-lysine (PDL) as a negative control, recombinant human MFAP4 [S2] or human plasma fibronectin as a positive control and incubated overnight at 4°C. Plates were washed and incubated with 10 mg/ml bovine serum albumin (BSA) for 1 h.

Real-time PCR

Total RNA was extracted from homogenized lung tissues or serum-starved BSMCs seeded for 24 h on ECM coating using TRIzol reagent according to the manufacturer's instructions. Total RNA from BSMCs derived from brionchial specimens was extracted using NucleoSpin RNA kit according to the manufacturer's instructions. One µg RNA was used for cDNA production. Reverse transcription was performed using M-MLV Reverse Transcriptase. Real-time PCR was performed using the TaqMan Universal PCR Master Mix and TaqMan Gene

Expression Assays specific for the given gene. The assay kits used were as follows: mGAPDH, Mm99999915_g1; mMFAP4, Mm00840681_m1; hGAPDH, Hs99999905_m1; hMFAP4, Hs00412974_m1; hCCL11, Hs00237013_m1.

In some experiments, cells were seeded in serum-free DMEM for 4 h to allow attachment. Subsequently, selective inhibitors of PI3K and MEK (LY294002 and PD98059, respectively) were added [S3-S4], and cells were collected after 24 h.

Adhesion assay

Cell adhesion was measured using the Vybrant Cell Adhesion Assay Kit (Molecular Probes). Briefly, cells were stained with calcein AM (1 µl/1 mln cells) in serum-free DMEM for 30 min at 37°C, seeded (100,000 cells/well) in uncoated or ECM-coated black 96-well plate and incubated for 1 h at 37°C. The plate was then washed with PBS and read. In some experiments, cells were pretreated with either RGD and DGR-containing peptides or anti-integrin antibodies for 30 min at room temperature prior to seeding. RGD-containing peptide recognizes and blocks the corresponding recognition motif on all αv integrins as well as α5β1, α8β1 and αIIbβ3 integrins. DGR-containing peptide is a non-blocking peptide used as a control. Integrin-blocking antibodies were anti-αv (clone L230), anti-β1 (clone P4C10), anti-αvβ3 (clone LM609) and anti-αvβ5 (clone P1F6). Isotype control antibody was used as a control for anti-integrin antibodies.

Proliferation assay

Cells were serum-starved for 24 h, resuspended in serum-free DMEM, seeded (10,000 cells/well) in an ECM-coated 96-well plate and incubated for 24 h at 37°C. Cells were then stained with BrdU for another 24 h at 37°C. Proliferation level was measured using BrdU Cell Proliferation Assay Kit according to the manufacturer's instructions.

In some experiments, cells were seeded in serum-free DMEM for 4 h to allow attachment. Subsequently, anti-integrin antibodies or selective inhibitors of PI3K and MEK (LY294002 and PD98059, respectively) were added for the rest of the incubation period. Isotype control antibody and DMSO were used as controls for anti-integrin antibodies and inhibitors, respectively.

Western blotting

Cells were serum-starved for 24 h, resuspended in serum-free DMEM, seeded in ECM-coated 6-well plates (500,000 cells/well) and incubated for various time points. After incubation, cells were washed with PBS and lysed in RIPA buffer with protease and phosphatase inhibitors. Equal amounts of samples were separated by SDS-PAGE and transferred to a polyvinylidene fluoride membrane. Blots were blocked with 5% nonfat dry milk in Tris-buffered saline (TBS)/0,1% Tween (TBST) for 1 h at room temperature and incubated overnight at 4°C with antibodies against GAPDH, integrin αv (clone M9), integrin β5, pFAK (T397) or FAK. After washing with TBST, the blots were incubated with goat anti-mouse Ig-HRP or goat anti-rabbit Ig-HRP for 1 h at room temperature. Proteins were detected using ECL reagents.

Flow cytometry staining of cell surface integrins

Near-confluent BSMCs were gently detached and harvested with alfazyme. Cells (200,000/tube) were resuspended in PBS with 2% FBS, stained with 10 µg/ml of anti-integrin antibodies or isotype control antibodies (Table S2) for 1 h on ice, washed with PBS and incubated with corresponding secondary antibodies (Table S1) for 30 min on ice. Cells were

acquired on LSRII flow cytometer (BD). Analysis was performed in FlowJo (TreeStar Inc, Ashland, OR, USA).

Table S1. Patient characteristics.

Patient ID	Sex	Age	Asthma status	Smoking
134	M	63	Asthmatic	Ex-smoker
135	M	69	Asthmatic	Ex-smoker
136	F	67	Asthmatic	Ex-smoker
137	F	64	Asthmatic	No
138	F	54	Asthmatic	No
142	M	70	Asthmatic	No
143	F	63	Asthmatic	Ex-smoker
325	F	64	Nonasthmatic	Yes
326	M	66	Nonasthmatic	No
327	M	58	Nonasthmatic	Yes
348	F	60	Nonasthmatic	Ex-smoker
349	F	68	Nonasthmatic	No
350	M	77	Nonasthmatic	Ex-smoker
352	M	24	Nonasthmatic	Yes
353	M	76	Nonasthmatic	Ex-smoker

F, female; M, male.

Table S2. List of antibodies used for flow cytometry.

Antibody	Clone	Host	Supplier
Integrin β1	P4C10	Mouse	Merck Millipore
Integrin αvβ5	P1F6	Mouse	Santa Cruz
Integrin αvβ3	LM609	Mouse	Millipore
Integrin β3	PM6/13	Mouse	Santa Cruz
Integrin β6	H-110	Rabbit	Santa Cruz
Integrin β8	H-160	Rabbit	Santa Cruz
Mouse IgG1 isotype control	-	Mouse	Dako
Normal rabbit IgG isotype control	-	Rabbit	Santa Cruz
Goat anti-mouse Ig-FITC	-	Goat	Dako
Goat anti-rabbit Ig-FITC	-	Goat	Dako

Fig. S1. MFAP4 deficiency has no effect on IL-4 or IL-5 but reduces IL-13 production. IL-4 (A), IL-5 (B) and IL-13 (C) levels were measured in BAL (left panel) and lung homogenates (right panel) in OVA-treated mice. n = 5-15. *$p < 0.05$, calculated by one-way ANOVA.

Fig. S2. MFAP4 does not contribute to IgE production. Allergen-specific IgE antibody levels do not differ between challenged groups in OVA or HDM model. n = 7-19.

Fig. S3. Integrin expression profile on BSMC surface. Figure shows relative expression of integrin β1, αvβ5, αvβ3, β3, β6 and β8 (solid histograms) together with isotype control signals (shaded histograms). Representative histograms of at least 3 independent experiments are shown. RFU, relative fluorescence units.

Fig. S1.

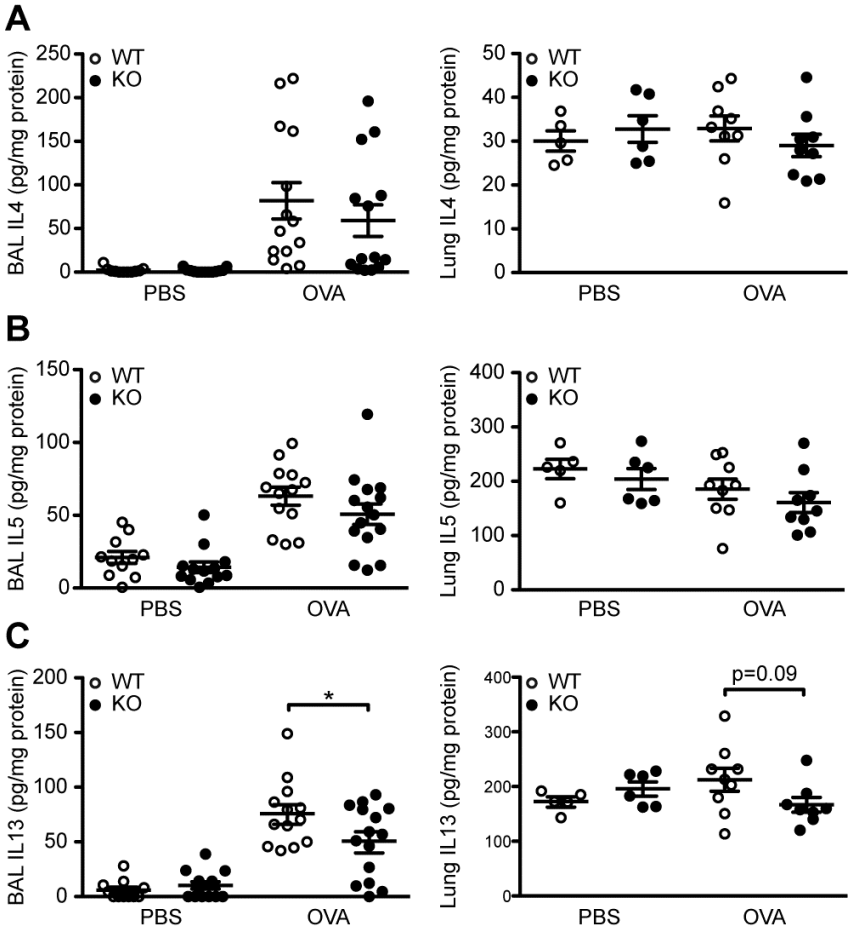
A
BAL IL4 (pg/mg protein)
Lung IL4 (pg/mg protein)
B
BAL IL5 (pg/mg protein)
Lung IL5 (pg/mg protein)
C
BAL IL13 (pg/mg protein)
Lung IL13 (pg/mg protein)
WT
KO
PBS
OVA
*
p=0.09

Fig. S2.

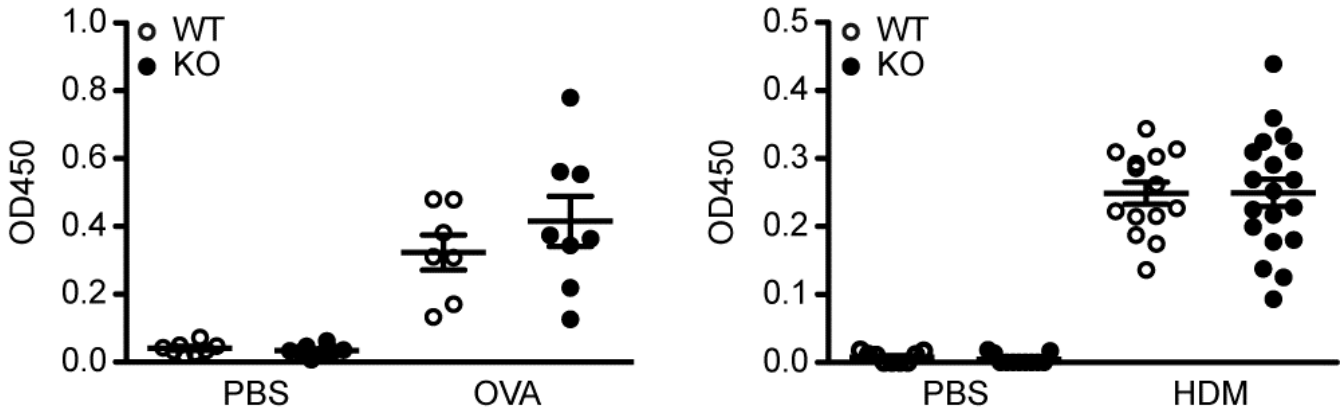
OD450
WT
KO
PBS
OVA
HDM

Fig. S3.

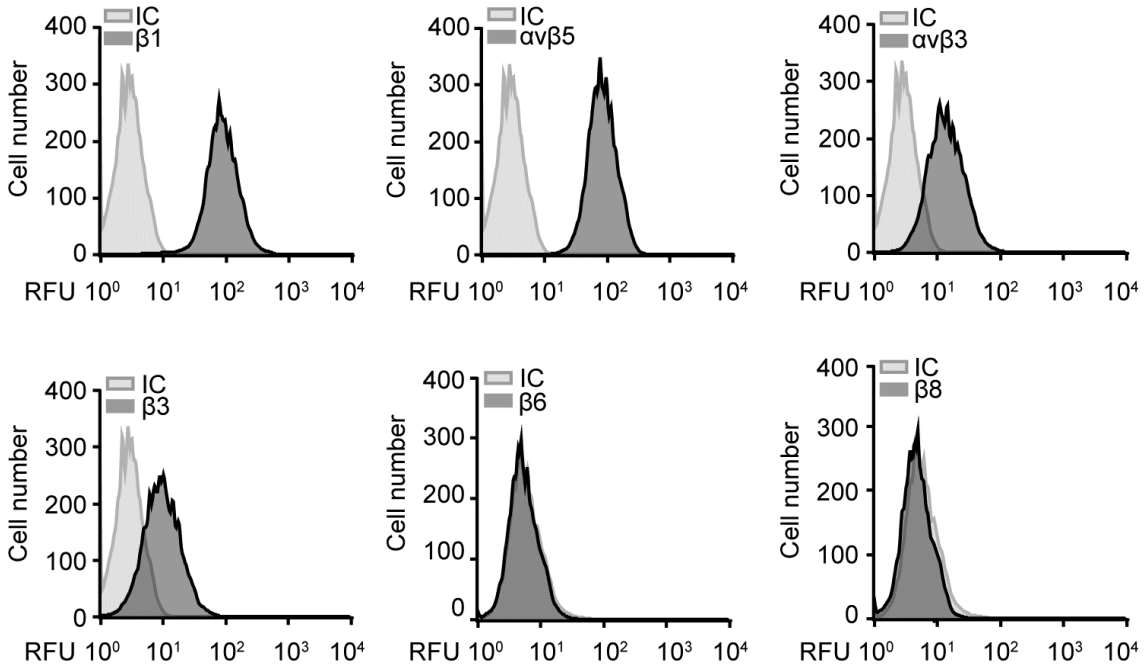

REFERENCES

S1. Schneider CA, Rasband WS, Eliceiri KW. NIH Image to ImageJ: 25 years of image analysis. Nat Methods 2012;9:671-675 doi: 10.1038/nmeth.2089.

S2. Saekmose SG, Schlosser A, Holst R, et al. Enzyme-linked immunosorbent assay characterization of basal variation and heritability of systemic microfibrillar-associated protein 4. PLoS One 2013;8(12):e82383 doi: 10.1371/journal.pone.0082383.

S3. Vlahos CJ, MatterWF, Hui KY, et al. A specific inhibitor of phosphatidylinositol 3-kinase, 2-(4-morpholinyl)-8-phenyl-4H-1-benzopyran-4-one (LY294002). J Biol Chem 1994;269(7):5241-8.

S4. Alessi DR, Cuenda A, Cohen P, et al. PD 098059 is a specific inhibitor of the activation of mitogen-activated protein kinase kinase in vitro and in vivo. J Biol Chem 1995;270(46):27489-94 doi: 10.1074/jbc.270.46.27489.